Journal of Molecular Catalysis B: Enzymatic 66 (2010) 325–331

Contents lists available at ScienceDirect

Journal of Molecular Catalysis B: Enzymatic

journal homepage: www.elsevier.com/locate/molcatb

An approach based on Density Functional Theory (DFT) calculations to assess the *Candida antarctica* lipase B selectivity in rutin, isoquercitrin and quercetin acetylation

Eduardo B. De Oliveira[a,*], Catherine Humeau[a,*], Elaine R. Maia[b], Latifa Chebil[a], Evelyne Ronat[a], Gerald Monard[c], Manuel F. Ruiz-Lopez[c], Mohamed Ghoul[a], Jean-Marc Engasser[a]

[a] Nancy Université, Laboratoire d'Ingénierie des Biomolécules (LIBio), ENSAIA-INPL, 2 av. de la Forêt de Haye, F-54500 Vandoeuvre-lès-Nancy, France
[b] Laboratorio de Estudos Estruturais Moleculares (LEEM), Instituto de Quimica, Universidade de Brasilia, 70904-970 Brasïlia, DF, Brazil
[c] Nancy Université, Groupe de Chimie et Biochimie Théoriques, SRSMC, CNRS, bd. des Aiguillettes, F-54506 Vandoeuvre-lès-Nancy, France

ARTICLE INFO

Article history:
Received 26 February 2010
Received in revised form 29 May 2010
Accepted 18 June 2010
Available online 30 June 2010

Keywords:
Bioprocesses
DFT
Docking
Flavonoid
Lipase
Molecular modelling
Substrate selectivity

ABSTRACT

Flavonoids are naturally occurring polyphenolic antioxidants of increasing biotechnological interest. Through lipase-catalyzed bioprocesses, they can be selectively converted into acylated derivatives displaying improved stabilities and bioavailabilites within nutritional or cosmetic formulations. In order to better understand the molecular basis for the selectivity in these bioconversions, we previously described the application of an enzyme–substrate docking protocol, which identified the most favourable orientations of the flavonoid glycosides isoquercitrin and rutin and their aglycon analogue quercetin within the catalytic cavity of the *Candida antarctica* lipase B (CALB). In the present work, we further applied quantum chemical calculations, based on the Density Functional Theory (DFT), in these enzyme–substrates complexes. The goal is to verify if the flavonoids OH groups reaching the CALB catalytic residues Ser105 and His224 are expected to form the ester bond that leads to the formation of the tetrahedral intermediate. According to the DFT results, after the transfer of the OH proton to the His224, an ester bond with the carbonyl carbon of the Ser105-bound acetate is expected to be formed for the glucose 6″-O of isoquercitrin and for the rhamnose 4‴-O for rutin. On the contrary, this ester bond is not expected to be formed with the B-ring 3′-O of quercetin. These theoretical results agree with available experimental data concerning the CALB-catalyzed acetylation of these three flavonoids and show that the reaction selectivity is influenced not only by the structural accessibility of the flavonoids OH groups to the catalytic residues, but also by the intrinsic chemical reactivity these OH groups.

1. Introduction

Flavonoids are a family of plant polyphenols whose molecules are characterized by a fifteen-carbon backbone structure formed by two aromatic rings (A- and B-rings), linked through three carbons that usually form an oxygenated heterocycle (C-ring). In nature, many of them occur as glycosides, with the flavonoid aglycon linked to a sugar moiety. In recent years, flavonoids have attracted strong interest due to their antioxidant properties and their beneficial health effects [1]. To be used as nutritional, cosmetic or pharmaceutical active ingredients, acylated derivatives of flavonoids are often preferred, as they display higher solubility and stability or improved biological properties when compared to the native molecules. Such flavonoids acylated derivatives are obtained by grafting one or several acyl groups on their poly-hydroxylated molecules [2,3]. As several biological activities of flavonoids depend on the number and position of their hydroxyl groups [4,5], it is important to control the regioselectivity of the acylation process, in order to preserve the hydroxyls responsible for these activities. Regioselectively acylated flavonoids can be efficiently synthesized in non-aqueous media with lipase as biocatalysts [6,7]. For the design of such processes, a key step is the selection of an enzyme able to catalyze the reaction between the flavonoid and the acyl donor with the desired regioselectivity. The biocatalyst can be selected among available microbial lipases or, alternatively, it may be a novel engineered lipase obtained by mutation of an existing enzyme. For now, due to the limited understanding of structural factors that determine the selectivity of the flavonoid acylation processes, a rational lipase selection or engineering approach can hardly be envisioned.

* Corresponding authors. Tel.: +33 03 83 59 57 84; fax: +33 03 83 59 57 78.
E-mail addresses: eduardobasilio@yahoo.com.br (E.B. De Oliveira), catherine.humeau@ensaia.inpl-nancy.fr (C. Humeau).

1381-1177/$ – see front matter © 2010 Elsevier B.V. All rights reserved.
doi:10.1016/j.molcatb.2010.06.009

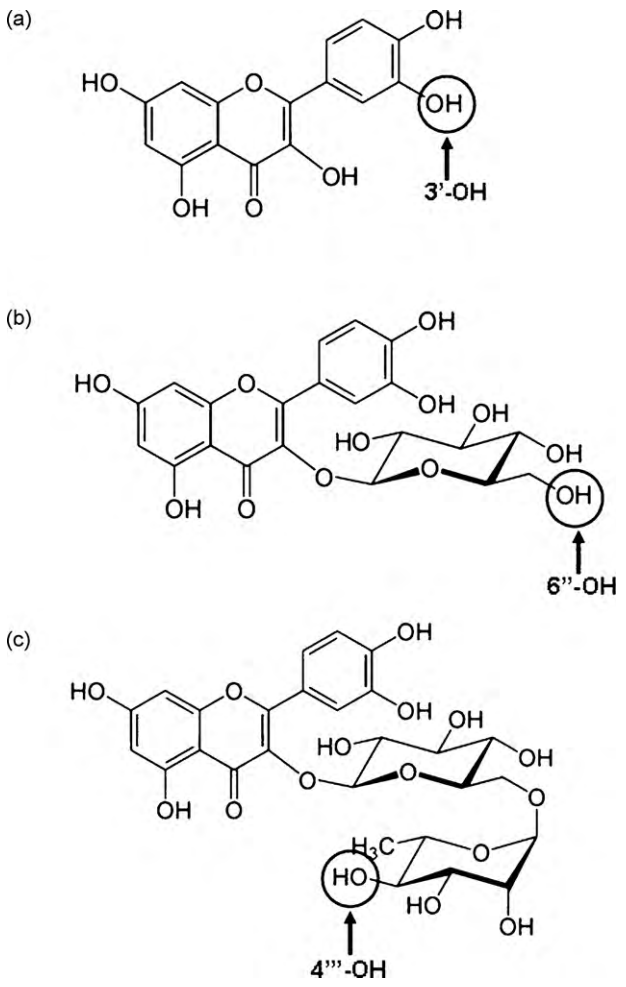

Fig. 1. Chemical structures of the flavonoids: (a) quercetin and its glycosylated analogues, (b) isoquercitrin and (c) rutin. The hydroxyl groups indicated by arrows are those accessible to the lipase catalytic residues of CALB, according to results from docking simulations [20,21] and/or experimental acetylation reactions [6,7].

During the past decade, molecular modelling techniques have been increasingly used to investigate the molecular basis of enzyme catalysis [8]. Applied to lipase-catalyzed reactions, numerous computational studies based on either molecular mechanics or *quantum* mechanics approaches contributed to assess the role of the catalytic pocket amino acids in controlling the bioconversion selectivity [9–15] or to clarify reaction mechanisms [16–18]. In particular, concerning the acylation of flavonoids, we previously related the application of an enzyme–substrate docking protocol to rationalize the regioselectivity of the lipase-catalyzed acetylation of quercetin and two of its glycosylated derivatives, isoquercitrin (quercetin-3-O-glucose) and rutin (quercetin-3-O-glucose-rhamnose), whose chemical structures are represented in Fig. 1. The modelling was based on the bi-bi ping-pong transesterification mechanism established for lipases [19], which involves two tetrahedral intermediates: the first one resulting from the nucleophilic attack of the catalytic serine on the acylating substrate, leading to the formation of an acyl-enzyme, and the second one coming from the nucleophilic attack of the acyl acceptor substrate on the acyl-enzyme, leading to the final product release. The tetrahedral intermediates are stabilized through hydrogen bonds formed between the oxyanion and the backbone amide hydrogens of the oxyanion hole residues (see Supplementary Data).

With the *Candida antarctica* lipase B (CALB) as biocatalyst, this docking protocol identified a single favourable binding mode for the glycosylated flavonoids isoquercitrin and rutin. They were found to bind through their flavan ring at the cavity entrance and their sugar moieties pointing towards the bottom of the pocket: for isoquercitrin, only the primary hydroxyl on the glucose part (6″-OH) is close to the catalytic His224 and to the Ser105-attached acetate, whereas for rutin the modelling identified a single secondary hydroxyl on rhamnose (4‴-OH) to be located near the catalytic residues [20]. When applied to quercetin, this protocol pointed out that this aglycon flavonoid docks in the CALB catalytic cavity with its B-ring 3′-OH group positioned at the pocket bottom, in close proximity to the catalytic residues Ser105 and His224 [21]. However, identifying the substrate hydroxyl groups that docks near the enzyme catalytic residues represents only the first step of a rational approach aimed at predicting the regioselectivity of flavonoids acetylation. In a following step, it is necessary to verify the reactivity of the formed lipase–flavonoid complex, by determining if the involved flavonoid hydroxyl is actually expected to form a covalent bond with the serine-bound acetate. This can only be theoretically evaluated by *quantum* chemical calculations [22].

Computational *quantum* chemical approaches, such as *ab initio* MP2 and Density Functional Theory (DFT), have been applied to investigate the pathway of lipase-catalyzed esterification/hydrolysis, based on a simplified model system of the lipase catalytic site [16]. Semi-empirical (AM1) and *ab initio* calculations were also used to study the enantioselectivity of secondary alcohols esterification and hydrolysis of their esters by *Burkholderia cepacia* lipase (BCL) [13]. In this study, starting from optimized enzyme–substrate complex, the model investigated the hydrogen transfer from histidine to serine oxygen during the formation of the ester and from the catalytic histidine to the alcohol oxygen during hydrolysis. Whereas in the case of the fast reacting substrate enantiomers all the identified binding modes were predicted to form the products, for the slow reacting ones, not all the binding modes were found as productive, according to the modelling results. In the present study we applied *quantum* chemical calculations based on DFT to analyze the reactivity of the binding modes for rutin, isoquercitrin and quercetin in the active site of CALB. Starting from the lipase–flavonoid complexes identified through a previously described docking protocol [20,21], model systems entailing the whole substrates molecules and key fragments of the lipase catalytic residues were constructed. DFT calculations were then performed on these mini-systems to determine if, after the transfer of the flavonoid OH proton to the His224 residue, an ester bond between the deprotonated oxygen and the acetate carbonyl carbon is expected to be established, leading to the formation of the second tetrahedral intermediate. For each of the three considered flavonoids, the propensity of formation of this ester bond results was analyzed and discussed in terms of variations of interatomic distances and atomic changes between the optimized model structures, after and before the flavonoid proton transfer to the catalytic histidine.

2. Modelling details

2.1. Computational resources

All the calculations were performed on a processor Intel Core Duo CPU 6550 2.33 GHz, equipped with 4.0 GB of RAM, using the DFT DMol^3 module of the software-package Materials Studio version 4.4 (*Accelrys, Inc.*).

2.2. Input molecular systems

The optimized Michaelis complexes consisting of the flavonoid rutin, isoquercitrin and quercetin docked in the acetyl-CALB were

obtained as described in our previous paper [20]. These complexes were the departure structures to construct the mini-systems for the DFT calculations. In order to enable the execution of *quantum* chemical calculations in practicable periods of time, the number of atoms in the molecular systems should be defined in function of the available computation power. Therefore, in this work, only the substrates molecules and the protein atoms directly implicated in the catalytic process were included in calculations, as follows: starting from the complexes above mentioned, the entire flavonoid, the entire Ser105-bound acetate and fragments of the catalytic residues were conserved. These kept residues fragments were the side chain carboxylate of Asp187, the imidazole ring of His224, the backbone and side chain of Ser105, the backbone –NH of Gln106, the backbone Cα and –NH and the entire side chain of Thr40. The other parts of the systems were simply rubbed out. The remaining free valences in the mini-systems were then filled with methyl groups ($-CH_3$). Simple hydrogen atoms could have been used to fill the free valences in order to further reduce the size of the systems [17,18]. Methyl groups were preferentially chosen to avoid the formation of artificial and undesired hydrogen bonds during the modelling procedure. The resulting systems thus included a total of 135, 115 and 94 atoms in the cases of rutin, isoquercitrin and quercetin, respectively. These systems were taken as input structures of the "reactant states" (RS) for the DFT structure optimizations.

2.3. DFT calculations

For the DFT optimizations of the RS structures, the spatial coordinates of the non-hydrogen atoms that constituted the protein backbone and the carbon atoms of the added methyl groups were kept frozen (fix constraint), in order to conserve the spatial disposition of the residues and substrates in the complexes [13,14]. The total charge of the systems was assigned as −1, due to the deprotonated Asp187 carboxylate. The exchange-correlation functional approximation GGA-PW91 [23] and the DNP basis set (Double Numerical with Polarization) [24] were used, with a global orbital cut-off of 3.7 Å. This basis set includes double-numerical basis functions together with polarization functions (that means, with angular momentum one higher than that of the highest occupied orbital in free atom). It has been demonstrated that DNP describes well the electronic behaviour of molecular systems containing hydrogen bond interactions, giving results comparable to those obtained with the more known Gaussian basis set 6-31G** [25]. The convergence tolerances were those corresponding to the "fine" criteria of DMol^3: 1.0×10^{-5} Ha (Hartree) for energy, 3.0×10^{-3} Å for the maximum displacement, and 4.0×10^{-3} Ha Å^{-1} for the maximum force.

Thereafter, starting from these optimized RS structures, the "intermediates structures" (Int) were constructed following the classical reaction mechanism of lipases: the flavonoid hydroxyl closest to the catalytic His224 was deprotonated, the His224:Nε atom was protonated and the acetate carbonyl carbon (Ace:C) was assigned as sp^3. After these modifications, the systems were again optimized, using the same methodology and parameters used for the corresponding RS optimizations. The energy differences (ΔE) between these intermediates (Int) and the reactant states (RS) were calculated by simple difference between the energies of the corresponding optimized structures [15], with the conversion factor 1 Ha/atom = 627.51 kcal mol^{-1}. Atomic charge distribution was determined by the Mülliken population analysis approach [26,27].

3. Results

Quantum chemical calculations based on the Density Functional Theory (DFT) were used to assess the propensity of the 4‴-OH of rutin, the 6″-OH of isoquercitrin and the 3′-OH of quercetin to form an ester bond with the carbonyl carbon of the Ser105-bound acetate. Indeed, for each flavonoid, these are the hydroxyl groups located in the close proximity of the CALB catalytic residues Ser105 and His224, according to previous docking simulations. Starting from the ES complexes, mini-systems were constructed, including the docked flavonoids, the acetate bound to the catalytic Ser105 and key fragments of the residues the catalytic triad residues (Ser105, His224 and Asp187) and of the oxyanion hole ones (Thr40 and Gln106). First, these mini-systems were optimized at the PW91/DNP level. Next, after the proton transfer from the closest flavonoid hydroxyl group to the His224, they were again optimized at the same level of theory. Variations in the key interatomic distances within the lipase catalytic residues and between the flavonoid and the acetylated lipase are shown in Table 1. The corresponding atomic charges on the involved atoms, calculated by the Mülliken population analysis approach, are reported in Table 2. The energetic variations are given in Table 3. In the following sections these DFT modelling results are analyzed in more details successively for rutin, isoquercitrin and quercetin.

3.1. Rutin binding mode

In the rutin mini-system (Fig. 2a and b), a first geometrical modification is the simultaneous decrease in the His224:Nε–Fla:H distance (from 2.21 Å to 1.03 Å) and the corresponding increase in the Fla:H–Fla:O distance (from 0.98 Å to 3.03 Å). This is accompanied by a change in the charge of the His224:Nε atom from −0.41 to −0.30. Together, these changes indicate that the proton transfer from the 4‴-OH hydroxyl group of rutin to the histidine actually results in the formation of a NH bond. There is also a proton transfer from His224 to Asp187: in the RS mini-system the His224:N_D proton form an hydrogen bond interaction with the deprotonated side chain carboxylate of the Asp187. In the Int mini-system, this proton is covalent bound to the Asp187, forming an hydrogen bond with the deprotonated His224:N_D. This suggests that the reaction follows a double proton transfer mechanism. Another noticeable change in the system is that the Fla:O–Ace:C distance decreases from 3.02 Å to 1.50 Å, which is compatible with formation of an ester bond between the flavonoid and the Ser105-bound acetate. Simultaneously, the Ser105:Oγ atom becomes more negative (atomic charge variation from −0.39 to −0.55) and the distance Ace:C–Ser105:Oγ increases from 1.33 Å to 1.51 Å, suggesting a weakening of the Ace:C–Ser105:Oγ bond in the formed intermediate. A slight increase in the Ace:C–Ace:O bond length (from 1.24 Å to 1.30 Å) and in the negative charge of the Ace:O atom (from −0.53 to −0.67) are also observed. In addition, the three canonical hydrogen bonds with the oxyanion hole (Ace:O···Thr40:OH, Ace:O···Thr40:NH and Ace:O···Gln106:NH) remain stable. All these findings suggest that the tetrahedral intermediate is expected to be formed when rutin docks within the CALB catalytic cavity with its 4‴-OH group in the neighbourhood of the catalytic triad residues Ser105 and His224. In this case, the calculated energy difference between the obtained tetrahedral intermediate (Int) and the initial non-covalent bound substrate (RS) mini-system structures is +13.8 kcal mol^{-1}.

3.2. Isoquercitrin binding mode

The behaviour of the isoquercitrin mini-system (Fig. 2c and d) is very similar to that observed for rutin. The proton transfer from the 6″-OH isoquercitrin hydroxyl group to histidine also results in the formation of a NH covalent bond: the His224:Nε–Fla:H distance decreases (from 2.38 Å to 1.04 Å), the Fla:H–Fla:O one increases (from 0.98 Å to 3.03 Å) and the His224:Nε charged varied

Table 1
Relevant interatomic distances and bond lengths (Å) in the reactant states (RS) and the intermediates (Int[a]) for the optimized mini-systems.

Interatomic distance or bond length	Rutin		Isoquercitrin		Quercetin	
	RS	Int[a]	RS	Int[a]	RS	Int[a]
Asp187:O_D–His224:H_{ND}	1.544	1.050	1.515	1.063	1.490	1.059
His224:H_{ND}–His224:N_D	1.093	1.580	1.091	1.506	1.116	1.624
His224:Nε–Ser105:Oγ	3.158	3.019	3.164	2.999	3.397	3.223
His224: Nε–Fla:H[b]	2.207	1.027	2.392	1.039	1.563	1.095
Fla:H[b]–Fla:O[b]	0.981	3.030	0.980	3.029	1.058	1.520
Fla:O[b]–Ace:C	3.017	1.501	3.409	1.452	3.616	3.020
Ace:C–Ser105:Oγ	1.333	1.509	1.337	1.549	1.346	1.351
Ace:C–Ace:O	1.239	1.300	1.242	1.314	1.232	1.230
Ace:O–Gln106:NH	2.061	2.318	1.876	1.932	1.994	1.947
Ace:O–Thr40:NH	2.132	2.237	2.208	2.369	3.216	3.175
Ace:O–Thr40:OH	1.987	1.722	1.793	1.658	2.625	2.857

[a] For rutin and isoquercitrin, "Int" corresponds to the tetrahedral intermediate, actually obtained through the DFT calculations. For quercetin, "Int" denotes the optimized mini-system after the deprotonation of the 3′-OH, which does not correspond to a tetrahedral intermediate.
[b] OH groups that reaches the catalytic residues His224 and Ser105: 4‴-OH of rutin, 6″-OH of isoquercitrin and 3′-OH of quercetin.

Table 2
Relevant Mulliken atomic charges in the reactant states (RS) and the intermediates (Int[a]) for the optimized mini-systems.

Atom	Rutin		Isoquercitrin		Quercetin	
	RS	Int[a]	RS	Int[a]	RS	Int[a]
Asp187:O_D	−0.606	−0.486	−0.620	−0.499	−0.614	−0.482
His224:H_{ND}	+0.295	+0.341	+0.295	+.0342	+0.313	+0.343
His224:Nε	−0.410	−0.299	−0.398	−0.273	−0.472	−0.359
Ser105:Oγ	−0.391	−0.551	−0.387	−0.530	−0.399	−0.414
Fla:H[b]	+0.311	+0.271	+0.298	+0.286	+0.347	0.324
Fla:O[b]	−0.511	−0.510	−0.526	−0.487	−0.510	−0.639
Ace:C	+0.564	+0.591	+0.544	+0.633	+0.531	+0.549
Ace:O	−0.534	−0.673	−0.561	−0.744	−0.494	−0.488
Gln106:NH	+0.256	+0.269	+0.257	+0.279	+0.248	+0.255
Thr40:NH	+0.224	+0.236	+0.217	+0.231	+0.179	+0.187
Thr40:OH	+0.295	+0.336	+0.369	+0.369	+0.284	+0.285

[a] For rutin and isoquercitrin, "Int" corresponds to the tetrahedral intermediate, actually obtained through the DFT calculations. For quercetin, "Int" denotes the optimized mini-system after the deprotonation of the 3′-OH, which does not correspond to a tetrahedral intermediate.
[b] OH groups that reaches the catalytic residues His224 and Ser105: 4‴-OH of rutin, 6″-OH of isoquercitrin and 3′-OH of quercetin.

from −0.40 to −0.27. The proton transfer from His224 to Asp187 also occurs. An ester bond is established between the flavonoid and the serine-bound acetate, as shown by the important reduction of the Fla:O–Ace:C distance (from 3.41 Å to 1.45 Å). For the formed tetrahedral intermediate, one also observes an increase in the distance between the Ser105:Oγ and the Ace:C atoms (from 1.34 Å to 1.55 Å), together with an increase in the negative charge on Ser105:Oγ (from −0.39 to −0.53). This indicates a weakening of the Ser105:Oγ–Ace:C covalent bond, which is favourable for the release of the acetylated product. The hydrogen bonds with the oxyanion hole (Ace:O···Thr40:OH, Ace:O···Thr40:NH and Ace:O···Gln106:NH) remain stable. The Ace:C–Ace:O bond length increases from 1.24 Å to 1.31 Å and in the negative charge of the Ace:O atom varies from −0.56 to −0.74. Thus, the tetrahedral intermediate is also expected to be formed for isoquercitrin, when it docks within the CALB catalytic cavity with its 6″-OH group in the close proximity of the catalytic triad residues. The corresponding energy difference between the obtained tetrahedral intermediate (Int) and the initial non-covalent bound substrate (RS) is calculated as +9.4 kcal mol^{-1}.

3.3. Quercetin binding mode

For quercetin, the DFT calculations results on the mini-systems display several differences when compared with those obtained for rutin and isoquercitrin (Fig. 2e and f). The proton transfer from the flavonoid 3′-OH to the His224:Nε results in the formation of an NH bond on histidine. Nevertheless, the variations in the His224:Nε–Fla:H distance (from 1.56 Å to 1.09 Å), in the Fla:H–Fla:O distance (from 1.06 Å to 1.52 Å) and in the His224:Nε atom charge (from −0.47 to −0.36) are slightly less pronounced than those observed for the two other flavonoids. Indeed, although covalently bound to the His224:Nε, the hydrogen keeps a hydrogen bond interaction with the deprotonated flavonoid oxygen, which does not happen with the two other analyzed flavonoid substrates. In addition, the distance between the quercetin deprotonated oxygen and the acetate carbonyl carbon (Fla:O–Ace:C) only slightly decreased from 3.62 Å to 3.02 Å, indicating that no covalent bond is established between these two atoms. The variations in the Ser105:Oγ–Ace:C and Ace:C–Ace:O distances (Table 1) and in the Ser105:Oγ and Ace:O charges (Table 2) are negligible.

Table 3
Energy values for the optimized mini-systems corresponding to the reactant state (RS) and the intermediates (Int[a]).

Flavonoid	Energy of reactant state systems (RS)/Ha	Energy of Intermediates systems (Int[a])/Ha	Energy difference/kcal mol^{-1}
Rutin	−3644.24791	−3644.22584	+13.8
Isoquercitrin	−3108.60354	−3108.58853	+9.4
Quercetin	−2497.87616	−2497.86065	+9.7

[a] For rutin and isoquercitrin, "Int" corresponds to the tetrahedral intermediate, actually obtained through the DFT calculations. For quercetin, "Int" denotes the optimized mini-system after the deprotonation of the 3′-OH, which does not correspond to a tetrahedral intermediate.

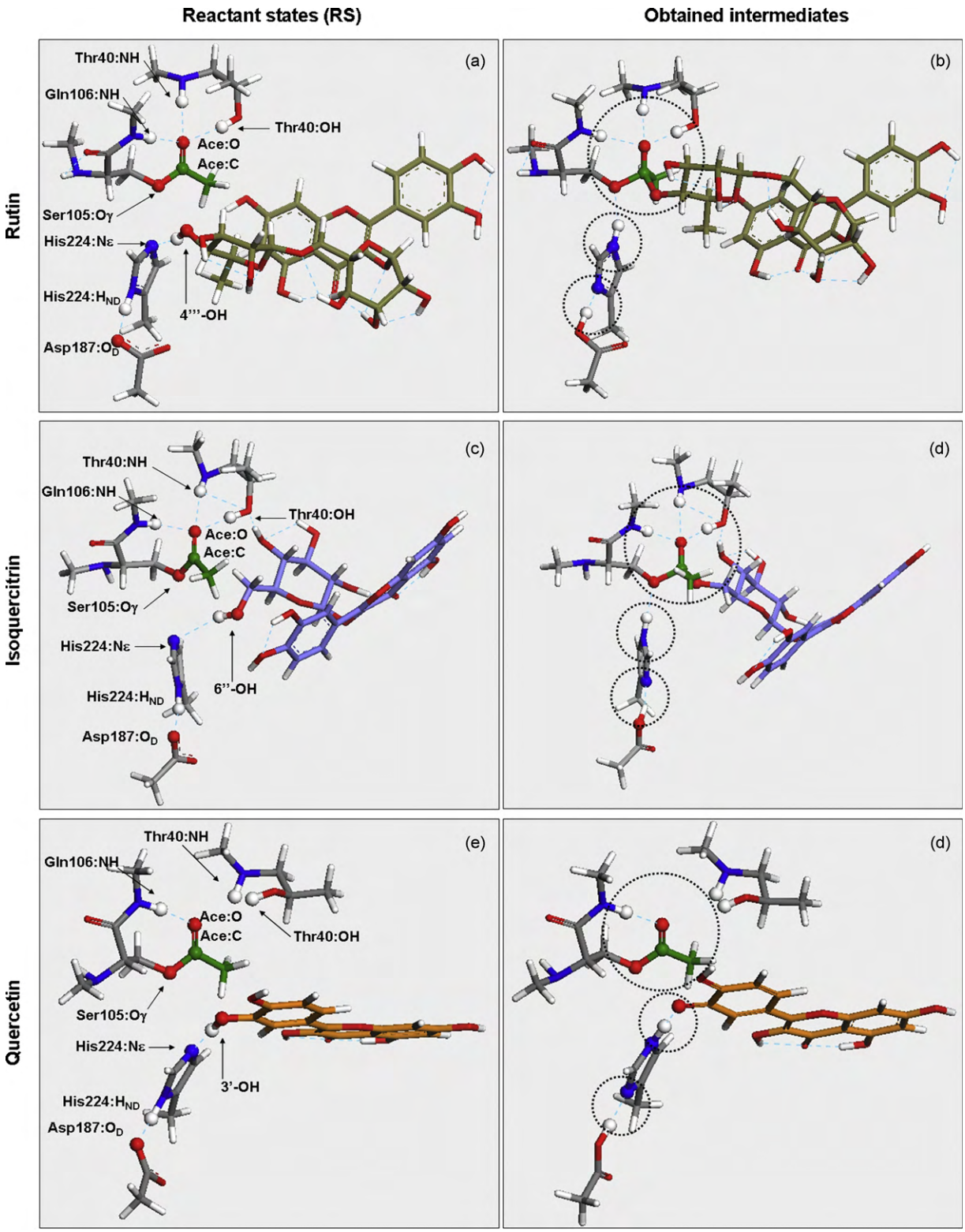

Fig. 2. Representation of the optimized mini-systems used for DFT calculations. In the first column, the reactant states (RS), which correspond to the Michaelis complexes. The atoms referred in the text are represented by spheres and identified by arrows. In the second column, the obtained intermediates structures (Int). The regions of the systems that underwent modifications are bordered with dashed circles. Hydrogen bonds are represented by dashed blue lines. All hydrogen atoms are coloured in white, oxygen in red and nitrogen in blue. Carbon atoms are coloured in grey for the amino acid fragments, green for the serine-bound acetate, greenish for rutin, purple for isoquercitrin and orange for quercetin. (For interpretation of the references to colour in this figure legend, the reader is referred to the web version of the article.)

Another important difference observed for quercetin is the greater values for the distances Ace:O–Thr40:NH and Ace:O–Thr40:NH, when compared to the values measured in rutin and isoquercitrin mini-systems (Table 1). As a consequence, two of the three catalytic hydrogen bonds between the acetate and the oxyanion hole residues are not formed. All these results further indicate that no tetrahedral intermediate is expected to be obtained, even if the quercetin can transfer its 3′-OH proton to the His224 residue.

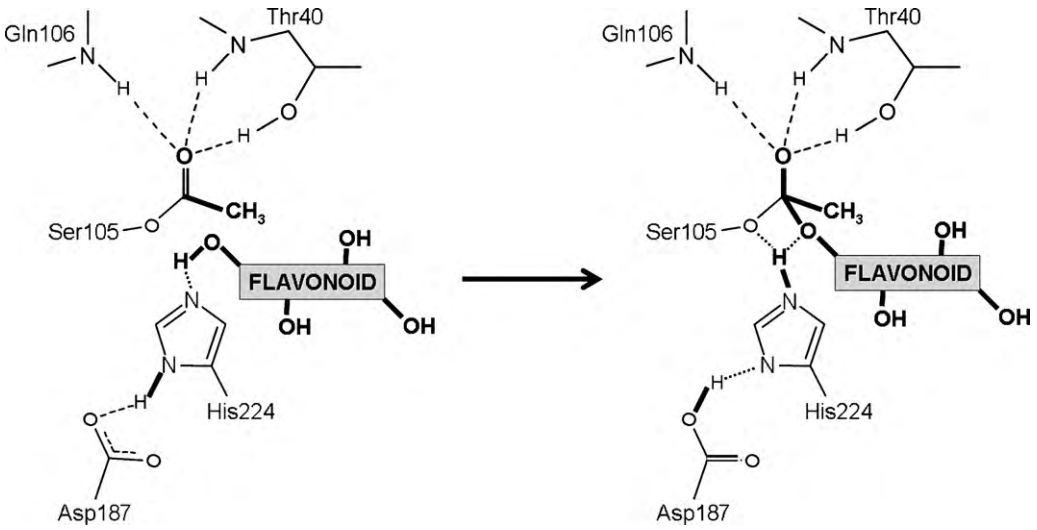

Fig. 3. Schematic representation of the tetrahedral intermediate formation, starting from the non-covalently bound flavonoids in the active site of CALB. According to our *quantum* chemical DFT results, the covalently bound intermediate is expected to be formed in the cases of rutin (4‴-OH) and isoquercitrin (6″-OH), but not in that of quercetin (3′-OH).

According to the calculations, the energy difference between the mini-systems after and before the quercetin 3′-OH proton transfer is +9.7 kcal mol^{-1}.

4. Discussion

In this work, Density Functional Theory (DFT) calculations were applied to evaluate the reactivity of rutin, isoquercitrin and quercetin, in their previously identified binding modes within the catalytic cavity of CALB. For these flavonoids, the hydroxyl groups that reach the catalytic residues Ser105 and His224 are the 4‴-OH, 6″-OH and 3′-OH, respectively (Fig. 1). Results were analyzed and discussed in terms of variations in bond lengths and atomic charges. According to the obtained models, after the proton transfer to the His224:Nε atom, an ester bond is expected to be established between the carbonyl carbon of the Ser105-bound acetate and the glucose 6″-O of isoquercitrin and the rhamnose 4‴-O of rutin. *A contrario*, no ester bond is expected to be formed between the 3′-O of the aglycon quercetin and the serine-bound acetate (Fig. 3). These theoretical predictions are in agreement with previously reported experimental data on the acetylation of the three flavonoids with CALB as biocatalyst [6,7]: when using vinyl acetate as acyl donor, both the glycosylated flavonoids were found to be regioselectively acetylated, rutin on the secondary 4‴-OH of its rhamnose moiety and isoquercitrin on the primary 6″-OH of its glucose moiety. Under the same conditions, no acetylated product was detected for quercetin.

For the glycosylated substrates DFT calculations also yielded the energy difference between the formed second tetrahedral intermediate and the initial Michaelis complexes: +9.4 kcal mol^{-1} for isoquercitrin-6″-acetate and +13.8 kcal mol^{-1} for rutin-4‴-acetate. These values are comparable to the energy difference of 9.6 kcal mol^{-1} between the tetrahedral intermediate and the non-covalently bound substrate, found by Hu et al. [16] for the serine deacetylation step. This theoretical study of methyl formate hydrolysis catalyzed by a serine hydrolase was performed on more simplified model system containing 21 atoms, where the catalytic triad was represented by formate anion (Asp), imidazole (His), and methanol (Ser), the oxyanion hole by two water molecule, and calculations were based on a post-HF method.

The present study provides some explanations for the reactivity differences observed between the sugar hydroxyl groups on the glycosylated flavonoids rutin and isoquercitrin on the one hand, and the aromatic hydroxyl on the aglycon quercetin, on the other hand. According to DFT calculations, a successful acetylation involves the stabilization of the formed tetrahedral intermediate through an efficient hydrogen bond network. For the productive isoquercitrin and rutin binding modes, five hydrogen bonds involving the catalytic residues and the substrates were found to stabilize the tetrahedral intermediate (Fig. 2a–d). On the contrary, after the deprotonation of the quercetin, hydrogen bond formation was less efficient for the obtained structure (Fig. 2e and f). This crucial role of the intermediate stabilization through hydrogen bonds was previously suggested to account for the enantiomeric preference of lipases in esterification and hydrolysis reactions [13,14]. In these studies, *quantum* chemical-based calculations indicated the formation of a higher number of hydrogen bonds, and molecular dynamics simulations showed that these interactions were more stable for the fast reacting substrate enantiomer. A previous more detailed energetic investigation of a lipase-catalyzed esterification mechanism had demonstrated that each hydrogen bond in the oxyanion hole contributes up to about 5 kcal mol^{-1} to the stabilization of the transition state, while that formed between the catalytic aspartate and histidine residues contributes up to about 6 kcal mol^{-1} [16].

The absence of ester bond formation with the docked quercetin can also be related to previous theoretical results demonstrating a reduced reactivity of the B-ring 3′-OH compared to the neighbouring 4′-OH. Using the DFT formalism at the B3LYP/6-31+G* level, Fiorucci et al. [28] reported that the free energy of deprotonation for the 3′-OH is 327.0 kcal mol^{-1}, while for the 4′-OH, the corresponding value is 318.2 kcal mol^{-1}. In another study, by applying higher level DFT calculations (B3LYP/6-31++G**), Antonczak [29] brought an explanation for these results: the deprotonation of the 4′-OH leads to a structure in which more favourable π-delocalization occurs over the flavonoid aromatic rings than in the case of the 3′-OH proton abstraction.

Finally, it is worthy to mention that the residues composing the CALB catalytic cavity walls were not included in the calculations, due to the restrictions commented in Section 2.2. Codorniu-Hernandez et al. [30–32] have demonstrated the great importance of the nature of the amino acid residues surrounding the active site of proteins for the recognition and the binding of flavonoids. According to their work results, these residues play a role in both the enthalpic (mainly hydrophilic residues) and entropic (mainly hydrophobic residues) components of the

protein–flavonoid complexes stabilization and in the polarization of the flavonoid hydroxyl groups. In that way, the inclusion of residues of the CALB cavity in the mini-systems could be useful to strength the results, because this can allow calculating highly precise enthalpy, entropy and free energy variations during the acetylation, with less frozen atomic coordinates. If the required computational apparatus is available, this could be achieved by two distinct ways: by the direct construction of larger mini-systems encompassing several residues surrounding the protein binding pocket for "gas-phase" QM calculations [32] or by the application of an hybrid QM/MM (*quantum* mechanics/molecular mechanics) approach [22]. In this last, the whole structure of the enzyme–substrate complex is kept, but only the atoms directly involved in the catalytic process are treated at the electronic level (QM approach); the remaining of the protein (and even the solvent molecules) is modelled through a classical force field (MM approach).

5. Summary and conclusions

Density Functional Theory (DFT) calculations were carried out on mini-systems representing three flavonoids (rutin, isoquercitrin and rutin) docked in the catalytic cavity of the lipase B from *C. antarctica*. In the calculations, were considered the OH group of each flavonoid that reaches the catalytic residues His224 and Ser105. The analysis of results showed that, once the flavonoid OH proton is transferred to the Nε atom of the His224 residue, an ester bond with the carbonyl C atom of the Ser105-bound acetate is expected to be formed for the rhamnose 4‴-O of rutin and for the glucose 6″-O of isoquercitrin. In contrast, no ester bond is expected to be formed with the B-ring 3′-O of quercetin. These theoretical results are in accordance with published experimental data concerning the CALB-catalyzed acetylation of these three flavonoids. Moreover they indicate that, when applying *in silico* approaches to predict the regioselectivity in lipase-catalyzed flavonoid acylation, not only which OH groups drawing near the catalytic residues must be considered, but also if these functional groups are chemically able to establish the ester bond leading to the second tetrahedral intermediate formation.

To further validate the predictive power of the described molecular modelling protocol for the regioselectivity in CALB-catalyzed acetylation of poly-hydroxylated molecules, a larger set of such compounds (aglycon and glycosylated flavonoids, phenolic acids, prostaglandins, sugars or others) should be studied, by combining this *in silico* approach and experimental verifications. Firstly, for each poly-hydroxylated compound, docking simulations would point out which hydroxyl group (OH) is more likely to reach the catalytic residues of the lipase. Next, DFT calculations would be applied to verify if the OH identified in the precedent step is actually able to form the tetrahedral intermediate (and hence, the ester product). Finally, the enzymatic reactions would be experimentally carried out with the aim of verify if the identified products – if any – correspond to those predicted by the combined docking/DFT methodology. After that, the existence of possible correlations between structural or energetic parameters in the models and the occurrence or not of the reaction may be investigated.

Appendix A. Supplementary data

Supplementary data associated with this article can be found, in the online version, at doi:10.1016/j.molcatb.2010.06.009.

References

[1] H. El Garras, Int. J. Food Sci. Technol. 44 (2009) 2512–2518.
[2] F. Mellou, D. Lazari, H. Skaltsa, A.D. Tselepis, F.N. Kolisis, H. Stamatis, J. Biotechnol. 116 (2005) 295–304.
[3] F. Mellou, H. Loutrari, H. Stamatis, C. Roussos, F.N. Kolisis, Process Biochem. 41 (2006) 2029–2034.
[4] L.M. Kabeya, A.A. De Marchi, A. Kanashiro, N.P. Lopes, C.H.T.P. Da Silva, M.T. Pupo, Y.M. Lucisano-Valim, Bioorg. Med. Chem. 15 (2007) 1516–1524.
[5] Y. Shimmyo, T. Kihara, A. Akaike, T. Niidome, H. Sugimoto, Biochim. Biophys. Acta 1780 (2008) 819–825.
[6] L. Chebil, C. Humeau, A. Falcimaigne, J.M. Engasser, M. Ghoul, Process Biochem. 41 (2006) 2237–2251.
[7] E. Xanthakis, E. Theodosiou, S. Magkouta, H. Stamatis, H. Loutrari, C. Roussos, F. Kolisis, Pure Appl. Chem. 82 (2010) 1–16.
[8] T.C. Bruice, Chem. Rev. 106 (2006) 3119–3139.
[9] T. Schultz, J. Pleiss, R.D. Schmid, Protein Sci. 9 (2000) 1053–1062.
[10] S. Tyagi, J. Pleiss, J. Biotechnol. 124 (2006) 108–116.
[11] M. Cammenberg, K. Hult, S. Park, ChemBioChem 7 (2006) 1745–1749.
[12] M.A.J. Veld, L. Franson, A.R.A. Palmans, E.W. Meijer, K. Hult, ChemBioChem 10 (2009) 1330–1334.
[13] S. Tomic, M. Ramek, J. Mol. Catal. B: Enzym. 38 (2006) 139–147.
[14] C.H. Kwon, J.Y. Jeong, J.W. Kang, Korean J. Chem. Eng. 26 (2009) 214–219.
[15] I. Vallikivi, L. Fransson, K. Hult, I. Järving, T. Pehk, N. Samel, V. Tõugu, L. Villo, O. Parve, J. Mol. Catal. B: Enzym. 35 (2005) 62–69.
[16] C.H. Hu, T. Brinck, K. Hult, Int. J. Quantum Chem. 69 (1998) 89–103.
[17] C. Branneby, P. Carlqvist, K. Hult, T. Brinck, P. Berglund, J. Mol. Catal. B: Enzym. 31 (2004) 123–128.
[18] M. Svedendahl, P. Carlqvist, C. Branneby, O. Allnér, A. Frise, K. Hult, P. Berglund, T. Brinck, ChemBioChem 9 (2008) 2443–2451.
[19] J. Uppenberg, M.T. Hansen, S. Patkar, T.A. Jones, Structure 2 (1994) 293–308.
[20] E.B. De Oliveira, C. Humeau, L. Chebil, E.R. Maia, F. Dehez, B. Maigret, M. Ghoul, J.M. Engasser, J. Mol. Catal. B: Enzym. 59 (2009) 96–105.
[21] E.B. De Oliveira, Molecular simulations applied to the lipase-catalyzed acetylation of flavonoids: influence of the lipase and flavonoid structures on the bioconversion regioselectivity, Ph.D. Thesis, Institut National Polytechnique de Lorraine (INPL), Nancy, France, 2009. Available from: <http://tel.archives-ouvertes.fr/tel-00452422/fr>.
[22] F.A. Friesner, V. Gullar, Annu. Rev. Phys. Chem. 56 (2005) 389–427.
[23] J.P. Perdew, Y. Wang, Phys. Rev. B 46 (1992) 6671–6687.
[24] B. Delley, J. Chem. Phys. 92 (1990) 508–517.
[25] Y. Inada, H. Orita, J. Comput. Chem. 29 (2007) 225–232.
[26] R.S. Mülliken, J. Chem. Phys. 23 (1955) 1833–1840.
[27] R.S. Mülliken, J. Chem. Phys. 23 (1955) 1841–1846.
[28] S. Fiorucci, J. Golebiowski, D. Cabrol-Bass, S. Antonczak, J. Agric. Food Chem. 55 (2007) 903–911.
[29] S. Antonczak, J. Mol. Struct. THEOCHEM 856 (2008) 38–45.
[30] E. Codorniu-Hernandez, A. Mesa-Ibirico, R. Hernandez-Santiestéban, L.A. Montero-Cabrera, F. Martinez-Luzardo, J.L. Santana-Romero, T. Borrmann, W.D. Stohrer, Int. J. Quantum Chem. 103 (2005) 82–104.
[31] E. Codorniu-Hernandez, A. Rolo-Naranjo, L.A. Montero-Cabrera, J. Mol. Struct. THEOCHEM 819 (2007) 121–129.
[32] A. Rolo-Naranjo, E. Codorniu-Hernandez, N. Ferro, J. Chem. Inf. Model. 50 (2010) 924–933.